Bending Contributions to Hydration of Phospholipid and Block Copolymer Membranes: Unifying Correlations between Probe Fluorescence and Vesicle Thermoelasticity

James C-M. Lee, Richard J. Law, and Dennis E. Discher*

School of Engineering and Applied Science, University of Pennsylvania, Philadelphia, Pennsylvania 19104

Received November 30, 2000. In Final Form: March 23, 2001

The temperature-dependent hydration of several pure, net-neutral membranes was studied by spectroscopic shifts of the amphiphilic probe 6-dodecanoyl-2-(dimethylamino)-naphthalene (LAURDAN). A calibration scale for local polarity was first established with LAURDAN in various organic solvents. For phosphatidylcholine membranes above the gel-phase temperature, the log(local polarity) was found to be inversely related to the bending-renormalized area elastic moduli. A novel self-assembled polymer membrane broadens the correlation, and the absence of any discontinuity in local polarity with temperature indicates that the polymer membrane is in a suitable fluid phase. Separate correlations between the log(hydraulic permeability × membrane thickness) and the bending modulus, but not the area elastic moduli, strongly suggest that local bending fluctuations of a membrane are coupled to membrane hydration. The results identify the importance of a collective response, membrane flexure, to a molecular-scale property, specifically, hydration.

Introduction

The basic driving force for aggregation of amphiphilic molecules (e.g., phospholipids, diblock copolymers) in aqueous media is the minimization of hydrophobic exposure to water. Lamellar phases and vesicles are not an uncommon result. Although membrane formation is certainly dependent on molecular architecture, fluctuations that grow into transient defects such as aqueous inclusions can also have an important role in determining overall membrane properties and stability. Hydration in the immediate vicinity of a given membrane interface would seem intuitively correlated with such properties. Moreover, the formation of defects and cavities at the membrane/water interface as well as in the interior hydrophobic core are also fundamental to mechanisms underlying bilayer polymorphism,[1] protein insertion into membranes,[2] and membrane fusion.[3] Further understanding of membrane hydration should therefore prove broadly relevant.

A polarity-sensitive amphiphilic fluorophore, such as 6-dodecanoyl-2-(dimethylamino)-naphthalene (LAURDAN), incorporates into a membrane and enables spectroscopic measurements of membrane polarity. Mechanistically, any water in the membrane appears as a strong dipole set against a low dielectric hydrophobic core; spectral shifts in LAURDAN fluorescence thus become coupled to water content in the membrane.[4] This, in turn, can be affected by thermodynamic variables. For example, a temperature increase tends to reduce the cohesiveness of membranes through the proliferation of defects and aqueous inclusions or hydrophobic cavities[5] with more water molecules penetrating and partitioning into the membrane. The local polarity of the membrane invariably increases. Likewise, at a membrane phase transition, surface-average interfacial tension, $\bar{\gamma}$, between the hydrophobic core and the membranes' aqueous environment dramatically decreases. This is associated with a sudden increase in the water content of the membrane; when LAURDAN is incorporated, it is now well-documented that more energy will be dissipated from fluorescently excited LAURDAN as additional surrounding H_2O dipoles are forced to align (Figure 1A). This manifests itself in a strong red-shift in LAURDAN's emission spectrum. To quantify this shift, Gratton and co-workers have defined the "generalized polarization", GP,[6] and widely applied their analyses to phase transitions of different phospholipid systems[4,6−9] as well as glycosphingolipid[10] and natural membranes.[11]

Other experimental techniques to determine water content in membranes have also been documented. Time-resolved fluorescence spectroscopy of 1-palmitoyl-2-[[2-[4-(6-phenyl-*trans*-1,3,5-hexatrienyl)phenyl]ethyl]carbonyl]-3-*sn*-phosphatidylcholine (DPH-PC) has been used to determine the degree of hydration in the acyl chain region together with acyl chain order.[12] Measurements of rigid-limit magnetic parameters of cholestane spin labels and 12-(9-anthroyloxy)stearic acid fluorescence have revealed water accessibility to the hydrophilic and hydrophobic loci of membranes, respectively.[13] A dual radiolabel

* To whom correspondence should be addressed. E-mail: discher@seas.upenn.edu.

(1) Turner, D. C.; Gruner, S. M. *Biochemistry* **1992**, *31*, 1356.
(2) Jähnig, F. *Proc. Natl. Acad. Sci. U.S.A.* **1983**, *80*, 3691.
(3) Siegel, D. P. *Biophys. J.* **1999**, *76*, 291.
(4) Parasassi, T.; Krasnowska, E. K.; Bagatolli, L.; Gratton, E. *J. Fluoresc.* **1998**, *8*, 365.
(5) Chong, P. L.; Tang, D.; Sugar, I. P. *Biophys. J.* **1994**, *66*, 2029.
(6) Parasassi, T.; De Stasio, G.; d'Ubaldo, A.; Gratton, E. *Biophys. J.* **1990**, *57*, 1179.
(7) Parasassi, T.; Stasio, G.; Ravagnan, G.; Rusch, R. M.; Gratton, E. *Biophys. J.* **1991**, *60*, 179.
(8) Bagatolli, L. A.; Gratton, E. *Biophys. J.* **1999**, *77*, 2090.
(9) Bagatolli, L. A.; Gratton, E. *Biophys. J.* **2000**, *78*, 290.
(10) Bagatolli, L. A.; Gratton, E.; Fidelio, G. D. *Biophys. J.* **1998**, *75*, 331.
(11) Parasassi, T.; Gratton, E.; Yu, W. M.; Wilson, P.; Levi, M. *Biophys. J.* **1997**, *72*, 2413.
(12) Ho, C.; Slater, S. J.; Stubbs, C. D. *Biochemistry* **1995**, *34*, 6188.
(13) Kusumi, A.; Subczynski, W. K.; Pasenkiewicz-Gierula, M.; Hyde, J. S.; Merkle, H. *Biochim. Biophys. Acta* **1986**, *854*, 307.

10.1021/la001678v CCC: $20.00
Published on Web 05/11/2001

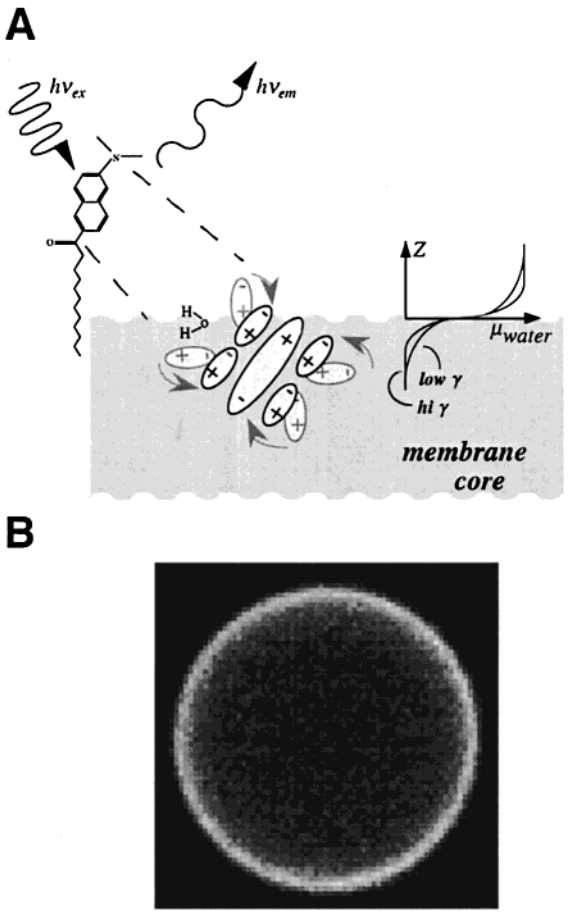

Figure 1. (A) Schematic illustration of the mechanism underlying LAURDAN's spectral shift in a membrane. LAURDAN possesses both an electron donor and an electron receptor, so that fluorescent excitation induces a large excited-state dipole. This strong dipole tends to locally align surrounding molecules (e.g., water), which dissipate a small fraction of the excited-state energy and shift the emission spectrum toward the red. As an initial concept, a membrane with a lower interfacial tension, γ, generally allows more water molecules to partition into the membrane, shifting LAURDAN's emission maximum further into the red. (B) Fluorescence image of LAURDAN incorporated into an OE7 vesicle. The edge-brightness of the ~10 μm diameter vesicle indicates that LAURDAN preferentially partitions into the membrane consistent with LAURDAN being extremely water-insoluble. Similar observations were made of LAURDAN incorporated into DMPC and SOPC vesicles.

centrifugation technique has also been applied to directly determine the amount of bound water in different membrane structures, such as the interdigitated, ripple, and gel structures.[14] Hydration at the lipid/water interface has also been examined by scattering methods.[15−17]

Theoretical approaches to membrane water content have added further insight. The partition coefficient for water into membranes has been predicted to be highly dependent on local lipid chain microstructure by lattice calculations.[18] Molecular dynamics (MD) simulations[19,20] have fortified this conclusion and motivated the development of analytical relationships between size selectivity and solute partitioning by use of scaled-particle theory.[21] Hydration of membranes as modulated by cholesterol has also been studied by MD.[22]

Although many aspects of water partitioning into membranes have been examined, relationships between partition coefficients and the thermomechanical properties of membranes have not been fully elucidated. In this work, we have used fluorescence spectroscopy of LAURDAN to focus on the hydration of three zwitterionic phospholipid membranes, 1-stearoyl-2-oleoyl-glycero-3-phosphocholine (SOPC), 1,2-dimyristoyl-*sn*-glycero-3-phosphocholine (DMPC), and 1,2-dierucoyl-*sn*-glycero-3-phosphocholine (DEPC), as well as a novel polymer membrane of ethyleneoxide$_{40}$-ethylethylene$_{37}$ (denoted OE7)[23] that expands the set of net-neutral amphiphiles. Spectroscopy was done in combination with micromanipulation measurements of the thermoelastic properties of single giant vesicles. Correlations that emerge between membrane polarity, permeability, thickness, and mechanical properties (i.e., bending and area expansion elasticity) shed light on the mechanism of membrane core hydration.

Materials and Methods

Chemicals. The diblock copolymer, OE7, was synthesized by Hillmyer and Bates.[23] Stock solutions of SOPC, DMPC, and DEPC from Avanti Polar Lipids, Inc. (Alabaster, AL) and LAURDAN from Molecular Probes were made in chloroform. Cyclohexane, dodecane, chloroform, cyclohexanol, 2-propanol, ethanol, and methanol were from Sigma.

Preparation of Labeled Vesicles. A trace amount (0.001 mol %) of LAURDAN was mixed with either polymer or lipid in chloroform, and preparation of vesicles was accomplished by film rehydration. Briefly, 20 mL of 4.0 mg/mL of either polymer or lipid with LAURDAN was uniformly coated on the inside wall of a glass vial. This was followed by evaporation of the chloroform under vacuum for 3 h. Final addition of nitrogen purged sucrose solution (250−300 mOsm) with minimal agitation led to spontaneous budding of vesicles off the glass wall and into the suspension.

Fluorescence Spectroscopy of LAURDAN. Spectroscopic measurements were accomplished with an SLM2000 spectrofluorometer (Spectronic Instruments, Newark, DE) outfitted with temperature control and Hg-lamp excitation. Energy dissipation from excited LAURDAN was calculated from the wavelengths of maximal excitation (λ_{ex}) and maximal emission (λ_{em}):

$$\Delta q = \frac{1}{\lambda_{ex}} - \frac{1}{\lambda_{em}} \quad (1)$$

Peak wavenumbers are used rather than spectral means because spectral peaks are reasonably symmetric and also because low wavenumber shoulders of emission peaks are uncertain because of scattering from the excitation beam. Calculation of the GP of LAURDAN follows the definition of Gratton and co-workers:[7] GP = $(I_B - I_R)/(I_B + I_R)$, where I_B and I_R are the intensities at λ_B and λ_R, respectively. λ_B and λ_R are the emission peaks at 5 and 60 °C, respectively.

Microscopy and Micromanipulation. Video microscopy was done with a Nikon TE-300 inverted microscope in either bright-field or phase contrast. Image collection through 10× or 20× objective lenses was accomplished through a CCD video camera mounted on the front port of the microscope. A custom manometer with pressure transducers (Validyne, Northridge, CA) was used for controlling and monitoring the pressure applied to the micropipet. Manipulation at various temperatures was performed in a custom-made thermal chamber calibrated to

(14) Channareddy, S.; Janes, N. *Biophys. J.* **1999**, *77*, 2046.
(15) McIntosh, T. J.; Simon, S. A. *Biochemistry* **1993**, *32*, 8374.
(16) König, S.; Pfeiffer, W.; Bayerl, T.; Richter, D.; Sackmann, E. *J. Phys. II* **1992**, *2*, 1589.
(17) Wiener, M. C.; White, S. H. *Biophys. J.* **1992**, *61*, 434.
(18) Marqusee, J. A.; Dill, K. A. *J. Chem. Phys.* **1986**, *85*, 434.
(19) Xiang, T.-X.; Anderson, B. D. *Biophys. J.* **1993**, *66*, 561.
(20) Marrink, S. J.; Berendsen, H. J. C. *J. Phys. Chem.* **1994**, *98*, 4115.
(21) Mitragotri, S.; Johnson, M. E.; Blankschtein, D.; Langer, R. *Biophys. J.* **1999**, *77*, 1268.
(22) Pasenkiewicz-Gierula, M.; Róg, T.; Kitamura, K.; Kusumi, A. *Biophys. J.* **2000**, *78*, 1376.
(23) Hillmyer, M. A.; Bates, F. S. *Macromolecules* **1996**, *29*, 6994.

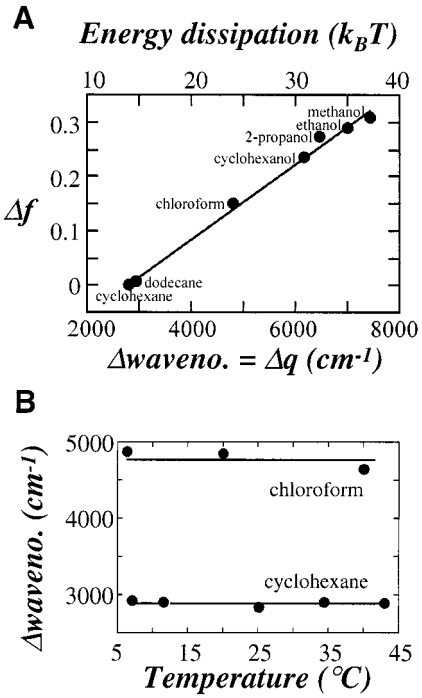

Figure 2. (A) Correlation between energy dissipation in LAURDAN fluorescence and solvent polarity. The wavenumber of the emission peak, q_{em}, is subtracted from that of the excitation peak, q_{ex}, to give $\Delta q = q_{ex} - q_{em}$. The polarity, Δf, of each solvent was calculated from its dielectric constant, ϵ, and refractive index, n, as $\Delta f = (\epsilon - 1)/(2\epsilon + 1) - (n^2 - 1)/(2n^2 + 1)$ (ref 6). (B) The energy dissipated from LAURDAN that is excited while dissolved in organic solvents, e.g., cyclohexane and chloroform, is essentially independent of temperature.

within ±1 °C. The area elastic modulus and the thermal expansivity of membranes were measured by micropipet methods.[24]

Fluorescence microscopy was generally done with a 40×, 0.75 NA air objective lens using a standard UV filter set. A 10× lens magnified the image through the side port onto a Photometrics (Tucson, AZ) CH360 cooled and back-thinned CCD camera controlled with Image Pro (Silver Springs, MD) software. The excitation lamp shutter (Uniblitz; Vincent Associates, Rochester, NY) was synchronous with a second shutter exposing the CCD; the typical exposure time was set between 200 and 300 ms.

Results and Discussion

Red-Shifted Emission of LAURDAN and Membrane Area Expansion. LAURDAN is very water-insoluble. As illustrated with the fluorescently edge-bright polymer vesicle of Figure 1B, LAURDAN predominantly incorporates into the membrane. Similar observations were made with DMPC and SOPC vesicles, as reported by others.[9] When LAURDAN integrates into membranes, its lauric acid chain provides a strong hydrophobic anchor into the membrane core (Figure 1), pulling the fluorescent moiety into the hydrophobic core beneath the lipid/water interface.[25] Fluorescence excitation leads to a localized charge separation that couples dissipatively to surrounding dipoles. Depending on the extent of this local coupling to solvent dipoles, LAURDAN emission is red-shifted, as illustrated by the series of pure organics in Figure 2A. Importantly, this fluorescence is essentially independent of temperature (Figure 2B) in such solvents. Hence, spectroscopic measurements of LAURDAN in a membrane as a function of temperature can be used as an indicator

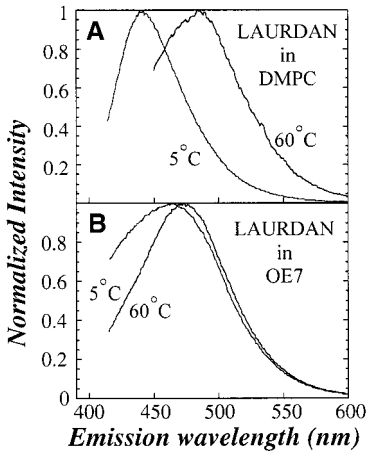

Figure 3. Emission spectra of LAURDAN in membranes of DMPC (A) and OE7 (B) when excited at 350 nm and measured at $T = 5$ or 60 °C. The emission peaks at these two temperatures were defined as λ_B and λ_R, respectively, for the calculation of generalized polarization, GP, at different temperatures. The emission spectra of LAURDAN in DMPC shows a red-shift of 40 nm from 5 to 60 °C, whereas LAURDAN in OE7 shows a red-shift of only 5 nm. The results indicate that the polarity of OE7 membranes does not increase significantly with temperature in comparison with DMPC membranes.

for changes in extrinsic factors, that is, the changing local polarity in the hydrophobic core near the lipid/water interface of a membrane, rather than factors intrinsic to the fluorophore.

The emission peak of LAURDAN in DMPC membranes is found to be red-shifted by ~40 nm when the temperature, T, is raised from 5 to 60 °C (Figure 3A) similar to the reports of others.[6] The result indicates that more energy is dissipated at the higher temperatures in the alignment of LAURDAN-local dipoles; the red-shift further implies that more water has penetrated into the DMPC membranes. In OE7 membranes, by contrast, LAURDAN exhibits a red-shifted emission of only ~5 nm under the same conditions (Figure 3B). However, relative to DMPC, the initial emission peak at 5 °C is red-shifted, suggesting more membrane-water content at the outset despite the minimal increase in hydration with temperature.

The GP, as normally defined by Gratton and coworkers,[7] decreases with increasing temperature. In contrast, the relative area, A/A_0, of membranes as measured by micropipet methods increases with temperature. To provide an initial perspective on the close relation between red-shifts in LAURDAN emission and membrane thermoelastic properties, useful definitions are made around a common datum. GP_0 is defined from the extrapolation of GP(T) to 0 °C; $GP_0 - GP$ thus yields a quantity which increases with T. A/A_0 has likewise been normalized by identifying A_0 as the vesicle area extrapolated to 0 °C, rather than using the room temperature area as typically done. With these simple redefinitions, both $GP_0 - GP$ and $A/A_0 - 1$ increase in roughly parallel fashion with T (Figure 4).

For DMPC membranes, a phase transition at 24 °C was found by both spectroscopic and micropipet methods (Figure 4A), consistent with previous reports.[6,24] For OE7 membranes, no clear phase transitions were observed, although weak increases in both $GP_0 - GP$ and $A/A_0 - 1$ were observed as a function of temperature (Figure 4B). Although previous calorimetric studies of *bulk* OE7 indicate a sharp transition within the lamellar phase at T as low as 50 °C, this is readily attributed to poly(ethylene oxide) (PEO) transformations that are extremely unlikely

(24) Evans, E.; Needham, D. *J. Phys. Chem.* **1987**, *91*, 4219.
(25) Chong, P. L.; Wong, P. T. *Biochim. Biophys. Acta* **1993**, *1149*, 260.

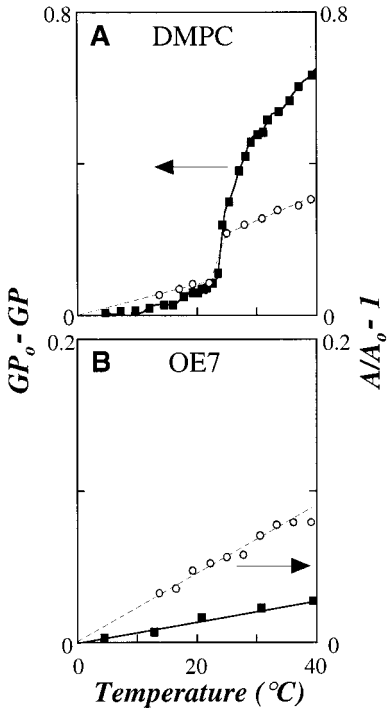

Figure 4. Comparison between the thermal expansion of membranes and the generalized polarization of LAURDAN for DMPC and OE7. GP_0 is defined by an extrapolation of GP to 0 °C, so that $GP_0 - GP$ increases with increasing temperature. Similarly, A/A_0, as obtained with micropipet manipulation methods, is normalized by extrapolating to $A/A_0 = 1$ at 0 °C. Both $GP_0 - GP$ and $A/A_0 - 1$ thus vanish at 0 °C. (A) For DMPC, both $GP_0 - GP$ and $A/A_0 - 1$ increase dramatically at the phase transition temperature of ~24 °C. Note that a steeper slope in $A/A_0 - 1$ corresponds to a steeper slope in $GP_0 - GP$. (B) By contrast, no phase transitions were revealed for OE7 membranes using both micropipet and spectroscopic methods.

with hydrated PEO.[23] Indeed, results of Figure 4 together with later results show no transition up to at least 60 °C. For either system at a given T, $GP_0 - GP$ and $A/A_0 - 1$ differ by less than a factor of 2−3. A common phenomenological basis is thus suggested and will be made more explicit below.

Membrane Hydration and Area Expansion with Temperature. A calibrated connection of GP to a physical measure of membrane hydration is necessary to more firmly establish a correlation with membrane area changes. In a pure solvent system, the energy dissipated from LAURDAN between excitation and emission depends strongly on solvent polarity, Δf, as calculated from the solvent's dielectric constant and refractive index (Figure 2A). Gratton and co-workers[6] reported a linear relationship analogous to that of Figure 2A between solvent polarity (Δf) and energy dissipation, Δq (cm^{-1}) (eq 1). For LAURDAN in various nonconjugated solvents, the data here has been fitted with

$$\Delta f = c_0 + c_1 \Delta q \qquad (2)$$

where $c_0 = -0.19$ and $c_1 = 6.9 \times 10^{-5}$ cm. Therefore, as commonly hypothesized, the spectral shift of LAURDAN in membranes seems likely to reveal the LAURDAN-local water content through the effect of water dipoles on the quantifiable effective local polarity Δf. Because of LAURDAN's amphiphilicity and size, Δf primarily reflects the water content immediately below the lipid/water interface to an approximate depth of 0.4 nm (approximate size of LAURDAN's naphthalene group). Importantly,

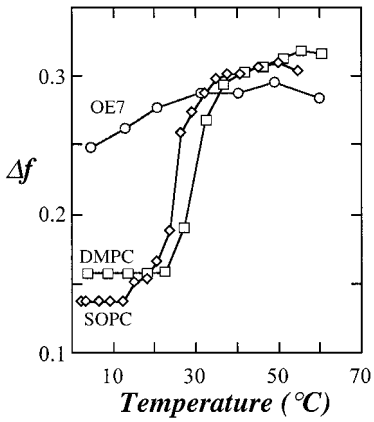

Figure 5. LAURDAN-local membrane polarity as a function of temperature. For the phospholipid membranes, SOPC and DMPC, membrane polarity remains unchanged with increasing temperature in the gel phase but does begin to increase dramatically near the phase transition temperatures of ~10 and ~24 °C, respectively. In the liquid-crystalline phase, the polarity increases weakly with increasing temperatures. This is also the case with the polymer membranes. In the liquid-crystalline phase, the slope of the polarity of the membranes with increasing temperature calculated from eq 2 is defined as the thermal polarizability, $d(\Delta f)/dT$.

however, the location of the probe is sufficiently far away from the lipid polar headgroups,[10] so that the dipolar relaxation process is independent of the chemical nature of the headgroup.[7]

For OE7, SOPC, and DMPC membranes, the LAURDAN-local polarity Δf versus T (Figure 5) was plotted explicitly. Below respective transition temperatures of 10 and 24 °C, SOPC and DMPC membranes appear to be in the gel phase where polarity and thus water content appear low and relatively uninfluenced by temperature. The results are consistent with a close-packed structure for the gel-phase bilayers. Just above their respective transition temperatures, the water content of these lipid membranes increases dramatically, clearly indicative of a phase transition where coexistence of gel−liquid domains leads to an enhanced permeation by water. Above about 30 °C, both DMPC and SOPC membranes appear to be in a more fluid liquid-crystalline phase with the water content of both membranes increasing more modestly with temperature.

OE7 membranes, in comparison, appear to be in a fluid phase over the entire range of T from 5 to 60 °C. At temperatures where the lipid membranes are in a gel phase, the water content of the OE7 membranes appears much closer to but still below the water content of the lipid membranes when in the fluid phase.

Local water content, defined as N water molecules interacting per probe amphiphile, and its changes can be crudely estimated from the dissipated energy, $\Delta\text{Energy} = hc\,\Delta q$, where h and c denote the usual universal constants. From 5 to 60 °C, the polarity, Δf, of the three membrane systems ranged from 0.15 to 0.3, which is equivalent to $\Delta\text{Energy} \sim 25-35\ k_BT$ (Figure 2A). As a simple model, one might assume that the energy dissipated in dipole alignment efficiently suppresses thermal rotations of energy $\sim{}^3/_2 k_BT$ per dipole. Molecular dynamics simulations of water molecules in phospholipid bilayers certainly suggest that such rotations are possible.[26] With suitable T (~300 K), we estimate N to vary from 16 to 23. This range compares well with results reported for molecular hydration of phospholipid membranes.[14]

(26) Tu, K.; Klein, M. L.; Tobias, D. J. *Biophys. J.* **1998**, *75*, 2147.

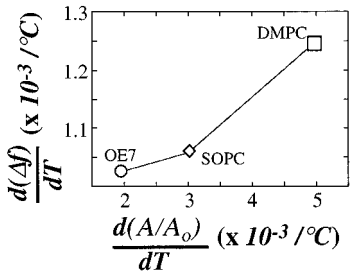

Figure 6. Monotonic correlation between thermal polarizability and thermal expansivity for membranes in the liquid-crystalline phase.

Thermal Expansivity of Membranes and LAURDAN-Local Polarity. Thermal expansion necessarily increases the aqueous area per molecule, and so probe hydration may be expected to increase concomitantly if not proportionally. The slope of the polarity, Δf, with respect to temperature, $\mathrm{d}(\Delta f)/\mathrm{d}T$, is defined here as the "thermal polarizability". At least within the liquid-crystalline phases, mean values of the thermal polarizabilities for the different membrane systems are found to increase with increasing thermal expansivities (Figure 6). A simple linear fit indicates that the probe-local polarity increases about 5−10-fold *less* than the effective expansion of the membrane. Together with the likely fact that N for any given system changes minimally from its low T value, probe hydration would appear to be closer than not to saturation.

LAURDAN-Local Polarity versus Projected Area Elasticity. A relationship between membrane hydration and the area elastic modulus of a membrane may be derived from basic considerations of water partitioning. The equilibrium partition coefficient, K, of a solute such as H_2O into a membrane is related to the change in the solute chemical potential associated with solute transfer into bilayers, $\Delta\mu_0$.

$$K = \exp(-\Delta\mu_0/k_\mathrm{B}T) \tag{3}$$

There are several factors contributing to $\Delta\mu_0$. The first factor is the work required to create a cavity for incorporating the solute into the bilayer. The second is the change in the interactions of the solute with its surroundings.[19] Regardless of the depth, z, into the membrane's hydrophobic core, $\Delta\mu_0$ has also been written as[21]

$$\Delta\mu_0 = W_\mathrm{b} - W_\mathrm{a} + \Delta\mu_{\mathrm{a-b}}^{\mathrm{sur}} \tag{4}$$

In this, W_b is the reversible work required to create a cavity for incorporating the solute into the bilayer, W_a is the reversible work required to create a cavity for incorporating the solute into the aqueous environment, and $\Delta\mu_{\mathrm{a-b}}^{\mathrm{sur}}$ is the difference in chemical potential of the solute in the aqueous phase and in the bilayer. In other words, $\Delta\mu_0$ involves the work to stretch and hydrate the core of the membrane, largely neglecting headgroups which, being polar, are readily hydrated and simply add a fraction to the lateral pressure that balances interfacial tension. As such, the stretching energy per water molecule can be approximated as $(\pi/2)K_\chi\xi^2$ where K_χ is a "suitable" area expansion modulus and $\pi\xi^2$ approximates the projected area of a water molecule and/or the insertion cavity.

There are at least two previously defined candidates for the area-stretching modulus, K_χ. One is the bare

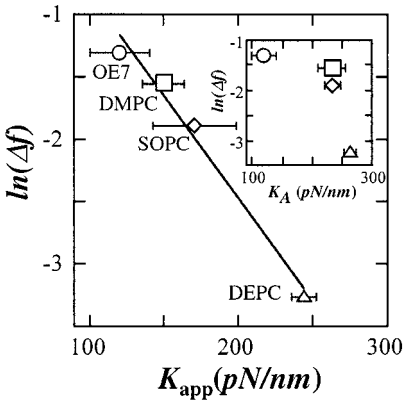

Figure 7. Correlation between membrane polarity, Δf, and the apparent area expansion modulus, K_app, for membranes: lipid (above the gel transition) or OE7. The inset shows no correlation with area expansion modulus, K_A. Data for K_app and K_A are those of Discher et al. (ref 37) and Rawicz et al. (ref 29).

cohesive modulus,[27] K_A, which Israelachvili[28] shows with an area-elasticity model to be related to the interfacial tension, γ, through $K_\mathrm{A} \approx 4\gamma$. Evans and co-workers[29] more recently calculated $K_\mathrm{A} \approx 6\gamma$ by treating the lipid bilayer core as a polymer brush; they also showed consistent with this experiment that K_A differs very little (≤5%) among a wide range of PCs. In contrast, the measurements of Δf for several PCs here show a significant variation (Figure 7). A second alternative K_χ is the area elastic modulus renormalized by ever-present thermally excited bending undulations at lowest order:[30,31]

$$K_\mathrm{app} \approx K_\mathrm{A} + K_\mathrm{A}^2 k_\mathrm{B}T/8\pi k_\mathrm{c}\bar{\tau} \tag{5}$$

where k_c (∼pN nm) is the membrane curvature modulus and $\bar{\tau}$ (∼ pN/nm) is the membrane tension. In practice, K_app is most directly measured in the high-tension regime ($\bar{\tau} \geq 0.5$ pN/nm) where longer wavelength undulations are smoothed out. Because the vesicles made here by hydration-swelling generally appear spherical as they form,[9,32] a moderate to high finite tension ($\bar{\tau} \sim 0.01-0.1\ K_\mathrm{A}$) is reasonable to expect.

Membrane stretching, as outlined above, ought to be related not only to $\Delta\mu_0 = -k_\mathrm{B}T \ln K$ but also, we conjecture here, to $-k_\mathrm{B}T \ln(\Delta f)$. Equations 3 and 4 would thus suggest that

$$k_\mathrm{B}T \ln(\Delta f) = -\frac{\pi}{2}(K_\mathrm{A} \text{ or } K_\mathrm{app})\xi^2 + \text{const} \tag{6}$$

where the constant term is assumed to be independent of membrane composition, at least above the gel transition. Plotting $\ln(\Delta f)$ against both K_A and K_app for a range of membranes shows a good correlation only with K_app (Figure 7). The finding that Δf shows a stronger variation between PCs is consistent with the idea that hydration of the hydrophobic core is not simply given by the interfacial tension (i.e., K_A). The present results imply foremost that hydration of disordered-phase membranes reflects both

(27) Evans, E. A.; Skalak, R. *Mechanics and Thermodynamics of Biomembranes*; CRC Press: Boca Raton, FL, 1980.
(28) Israelachvili, J. *Intermolecular and surface forces*, 2nd ed.; Academic Press: New York, 1991; Chapter 17.
(29) Rawicz, W.; Olbrich, K. C.; McIntosh, T.; Needham, D.; Evans, E. *Biophys. J.* **2000**, *79*, 328.
(30) Helfrich, W.; Servuss, R.-M. *Nuovo Cimento* **1984**, *D3*, 137.
(31) Evans, E.; Rawicz, W. *Phys. Rev. Lett.* **1990**, *64*, 2094.
(32) Lee, J. C.-M.; Bermudez, H.; Discher, B. M.; Sheehan, M. A.; Won, Y.-Y.; Bates, F. S.; Discher, D. E. *Biotechnol. Bioeng.* **2001**, *73*, 135.

the lateral cohesiveness and the bending rigidity. The quantitative correlation between $\ln(\Delta f)$ and K_{app} was fit to

$$\ln(\Delta f) = c_2 + c_3 K_{app} \quad (7)$$

where $c_2 = 0.81$ and $c_3 = -0.016$ (nm/pN).

The numerics of the correlation above may prove helpful in estimating membrane elastic properties from LAURDAN spectra. More importantly, eq 6 can be combined with eq 7 to estimate the underlying length scale, ξ, in $k_BT \ln[\exp(-c_2)\,\Delta f] = -(\pi/2)K_{app}\xi^2$, where $k_BT \approx 4$ pN nm (at $T \approx 296$ K). The correlation thus yields the approximate stretching dimension needed for the insertion of a water molecule, $\xi = \sqrt{4(2/\pi)c_3} \approx 0.2$ nm $= 2$ Å. As might be expected, the projected stretched area should be of the same order as or even greater than the size of a water molecule.

Permeation versus Bending Elasticity. There are at least two possible rate-limiting steps in the transport of water across a membrane. Transport in the interfacial region between the membrane and the aqueous solution could be rate-limiting. Diffusion in the nonpolar interior of the membrane could, alternatively, provide the maximum impedance.[33] The overall resistance of these transport processes may therefore be summed in series as[34]

$$\frac{1}{P_h} = \frac{2l}{D_{sm}} + \frac{d}{DK'} \quad (8)$$

where P_h is the hydraulic permeability, l is the width of each interfacial region containing the polar headgroups of the lipids, D_{sm} is the diffusion coefficient across the interfacial region from the aqueous solution into the membrane, d is the thickness of the hydrophobic core, D is the diffusion coefficient of water within the hydrophobic core, and K' is the mean partition coefficient for water into the hydrophobic core. K' is more restrictive in its assignment than K in eq 3 and is again logarithmically related (per eq 4) to the reversible work needed to partition water molecules from the interface into the hydrophobic core (W_b') and so forth.

The first term in eq 8 describes the interfacial region between lipid and water. Interfacial roughness associated with relative displacements or protrusions of bilayer molecules has already been assessed,[15−17,35] and the hydration of this interface as governed by an effective interfacial tension has been described theoretically.[36] In comparison, however, to the low diffusivity and the small partition coefficient for water into the hydrophobic core, resistance in the water/lipid interface (i.e., the first term in eq 8) is expected to be negligible.[33] If D is assumed invariant for different membranes, eq 8 plus eqs 3 and 4

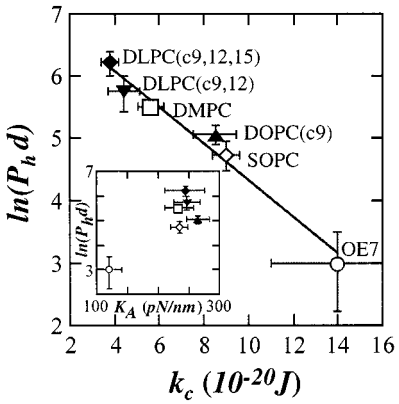

Figure 8. Correlation between permeability (P_h) × membrane thickness (d) and bending modulus, k_c, for a range of net-neutral liquid-crytalline phase lipid and OE7 membranes. The inset shows no correlation with the area expansion modulus, K_A. Data for k_c, K_{app}, K_A, and d are those reported by either Discher et al. (ref 37) or Rawicz et al. (ref 29). Data for P_h were taken from Olbrich et al. (ref 38), (for OE7) Discher et al. (ref 37), and (for DMPC) Bloom et al. (ref 39).

suggest an exponential dependence of $P_h d$ on W_b':

$$\ln(P_h d) \propto -W_b' \quad (9)$$

Water transport across a membrane thus appears intimately related to the work required to create a cavity in the bilayer. Indeed, Figure 8 shows for the best-characterized membranes that $\ln(P_h d)$ correlates most directly with bending through k_c as opposed to K_A (inset to Figure 8) or K_{app} (not shown). These results, therefore, suggest that the permeability of a membrane involves bending of a membrane. In comparison, local hydration of the thin interfacial region (perhaps ∼0.4 nm for lipid) near the aqueous interface of a hydrophobic core also reflects bending but through the bending-renormalized area elastic modulus (i.e., a combination of K_A and k_c).

Conclusions

The present study of a diverse set of pure-component bilayers, lipid as well as copolymer, indicates that membrane hydration, a very molecular-scale property, correlates well with an area elastic response that incorporates bending fluctuations of a membrane. Subsequent permeation of a membrane by a water molecule likewise correlates with bending of the membrane. The results suggest that the interaction of a water molecule with the hydrophobic core and the effective volume of a cavity accommodating a water molecule are, in principle, no different for different membranes. Ultimately, these findings may provide insight into the insertion of other compounds such as proteins into membranes as well as membrane fusion.

Acknowledgment. We thank Professor Frank S. Bates for his generosity in providing us with the diblock copolymers and Professor Daniel A. Hammer for use of the SLM2000 spectrofluorometer as well as general discussions about polymer membranes. This work was funded in part by NSF-MRSEC and NSF-PECASE grants to D. E. Discher.

LA001678V

(33) Fettiplace, R.; Haydon, D. A. *Physiol. Rev.* **1980**, *60*, 510.
(34) Zwolinski, B. J.; Eyring, H.; Reese, C. E. *J. Phys. Colloid Chem.* **1949**, *53*, 1426.
(35) Egberts, E.; Berendsen, H. J. C. *J. Chem. Phys.* **1988**, *89*, 3718.
(36) Lipowsky, R. In *Handbook of biological physics. Structure and dynamics* of *membranes*; Lipowsky, R., Sackmann, E., Eds.; Elsevier Science B.V.: Amsterdam, 1995; Vol. 1B, Chapter 11.
(37) Discher, B. M.; Won, Y.-Y.; Ege, D. S.; Lee, J. C.-M.; Bates, F. S.; Discher, D. E.; Hammer, D. A. *Science* **1999**, *284*, 1143.
(38) Olbrich, K.; Rawicz, W.; Needham, D.; Evans, E. *Biophys. J.* **2000**, *79*, 321.
(39) Bloom, M.; Evans, E.; Mouritsen, O. G. *Q. Rev. Biophys.* **1991**, *24*, 293.